

# Nonequilibrium Response Theory: From Precision Limits to Strong Perturbation

Ruicheng Bao<sup>1,\*</sup> and Shiling Liang (梁师翎)<sup>2,3,4,†</sup>

<sup>1</sup>*Department of Physics, Graduate School of Science, 7-3-1,  
The University of Tokyo, Hongo, Bunkyo-ku, Tokyo 113-0033, Japan*

<sup>2</sup>*Center for Systems Biology Dresden, 01307 Dresden, Germany*

<sup>3</sup>*Max Planck Institute for the Physics of Complex Systems, 01187 Dresden, Germany*

<sup>4</sup>*Max Planck Institute of Molecular Cell Biology and Genetics, 01307 Dresden, Germany*

Understanding the response of nonequilibrium systems to external perturbations remains a fundamental challenge in statistical physics. Here, we prove a novel universal bound stating that the response precision for state observable is fundamentally constrained to 1/2 under single edge or vertex perturbations, independent of system size. Furthermore, we develop exact relations connecting responses to perturbations of arbitrary strengths, extending nonequilibrium response theory beyond the weak-perturbation regime. Through response equalities we also provide a novel physical interpretation of response sensitivity and recovers bounds previously obtained using non-trivial graph-theoretical methods. Our results provide a general mathematical framework applicable across diverse nonequilibrium systems and offer design principles for optimal sensing and information processing in biochemical systems.

*Introduction.*— Fluctuation-response relations are cornerstones of statistical physics, fundamentally linking a systems' intrinsic fluctuations to its response to external perturbations. While fluctuation-dissipation theorems provide a complete framework near equilibrium [1], real-world systems such as biological systems operate far from equilibrium to achieve functions like signal processing and biochemical regulation [2–5], necessitating new theoretical tools for both fluctuations and responses in nonequilibrium settings.

Recent advances in stochastic thermodynamics have established a powerful framework for analyzing nonequilibrium systems at mesoscopic scale [6]. On the relation between fluctuation and response, general inequalities for both stationary and non-stationary cases were derived in [7] using stochastic trajectories and information theory. A parallel route uses algebraic graph theory to build thermodynamic bounds on steady-state responses [8–11]. More recently, identities and thermodynamic bounds were developed for response in nonequilibrium steady states, ranging from responses of steady-state distribution, currents to general observables [7, 12–20].

Despite these developments, a comprehensive framework for the response of nonequilibrium steady state remains incomplete. Firstly, existing non-equilibrium fluctuation-response bounds mainly focus on trajectory-wise observables [7, 16, 17, 20–24]. Such trajectory-wise observables are typically resource-intensive to measure experimentally. In contrast, state observables are more experimentally accessible as their statistical moments converge faster in both experimental sampling and numerical simulations. While recent work has explored bounds on state observable responses, these efforts have

been limited to specific observables and network topologies [11, 25]. A universal bound applicable to all state observables, independent of network architecture, remains largely unexplored. Second, most existing response theories, whether equilibrium or nonequilibrium, are limited to weak perturbation regime, with only limited exploration of finite perturbation bounds. However, practical applications often involve finite perturbations [26, 27], calling for a general framework that can address perturbations of arbitrary strength.

In this Letter, we address both challenges by establishing two fundamental results. First, we prove a universal bound stating that for any state observable, the ratio of response strength to standard deviation under single edge or vertex perturbation is constrained by 1/2. This saturable bound reveals fundamental physical limits on response precision that are independent of system size, timescales, and network architecture. Second, we derive exact identities linking finite and infinitesimal perturbation responses, extending nonequilibrium response theory beyond the linear regime. Our approach leverages mean first passage times (MFPT) to provide direct physical insight - through this lens, we obtain an elegant derivation of previously known bounds that were originally established through graph-theoretical method [8, 11]. We further establish novel bounds for current response, revealing its intrinsic connection to edge activities. Finally, we demonstrate these universal bounds in a minimal biochemical sensing model, illustrating their practical relevance for cellular information processing.

*Setup.*— We consider a continuous-time Markov process with  $N$  discrete states. The dynamics of the system is determined by a transition rate matrix  $W$  whose off-diagonal element  $W_{ij}$  denotes the transition rate on the edge  $e_{ij}$  from state  $j$  to state  $i$ . Its diagonal elements are defined as  $W_{ii} = -\sum_{j(\neq i)} W_{ji}$ . Assuming that  $W$  is irreducible ensures the existence of a steady-state probability distribution  $\boldsymbol{\pi} = (\pi_1, \dots, \pi_N)^T$  satisfying  $W \cdot \boldsymbol{\pi} = \mathbf{0}$ .

To formalize perturbations and responses, we

\* Corresponding author: ruicheng@g.ecc.u-tokyo.ac.jp

† Corresponding author: shiling@pks.mpg.de

parametrize the transition rates following [7, 8] as

$$W_{ij} = e^{-(B_{ij} - E_j - F_{ij}/2)} \quad (1)$$

where we set  $k_B T = 1$  for convenience. The kinetics is characterized by three types of parameters: vertex parameters  $E_j$  corresponding to energy well depths, symmetric edge parameters  $B_{ij} = B_{ji}$  representing barrier heights, and asymmetric edge parameters  $F_{ij} = -F_{ji}$  describing driving forces. The system is driven out of equilibrium when the sum of driving forces along any cycle (the cycle affinity  $F_c = \sum_{e_{ij} \in c} F_{ij}$ ) is non-zero. Below we analyze how physical observables respond to perturbations in these parameters.

*Steady-state response equalities and bounds*— Having established this parametrization of the nonequilibrium steady states, we now analyze how such states respond to perturbations of these parameters. Our analysis builds on a fundamental relation between steady-state responses and MFPTs [28–30]. For any parameter  $\theta$  associated with the transition matrix, this relation takes the form:

$$\frac{\partial \ln \pi_k}{\partial \theta} = \sum_{i,j (i \neq j)} \pi_j \frac{dW_{ij}}{d\theta} (\langle t_{kj} \rangle - \langle t_{ki} \rangle), \quad (2)$$

where  $\langle t_{ij} \rangle$  denotes the mean first-passage time from state  $j$  to state  $i$ . For  $i \neq j$ ,  $\langle t_{ij} \rangle$  represents the average time for the system to first reach state  $i$  starting from state  $j$ , while we set  $\langle t_{ii} \rangle = 0$ . Applied to perturbations of individual edges, this relation yields:

$$\frac{\partial \ln \pi_k}{\partial B_{mn}} = (\langle t_{kn} \rangle - \langle t_{km} \rangle) j_{nm}, \quad (3a)$$

$$\frac{\partial \ln \pi_k}{\partial F_{mn}} = (\langle t_{kn} \rangle - \langle t_{km} \rangle) \frac{A_{mn}}{2}, \quad (3b)$$

where  $j_{nm} = W_{nm}\pi_m - W_{mn}\pi_n$  is the steady state probability current from state  $m$  to state  $n$  and  $A_{mn} = W_{mn}\pi_n + W_{nm}\pi_m$  is the edge activity of  $e_{mn}$ . The response equalities based on MFPTs recover a key result from [15]: edge-symmetric perturbations yield non-zero responses only when the perturbed edge carries a non-zero steady-state current, a condition stronger than non-equilibrium. Moreover, a known result of vertex perturbation obtained from non-trivial graph-theoretical method [8] is recovered from Eq. (2) as

$$\frac{\partial \ln \pi_k}{\partial E_m} = \pi_m - \delta_{km}, \quad (4)$$

where  $\delta_{km}$  is the Kronecker delta. Here,  $\sum_i W_{ij} \langle t_{ki} \rangle = \delta_{jk} / \pi_j - 1$  and  $\sum_i W_{ij} = 0$  have been used.

Note that Eqs (3a) and (3b) relate the response to the difference in MFPTs between the two ends of the perturbed edge. For states at the ends of the perturbed edge, we find:  $\partial_{B_{mn}} \ln \pi_m = \langle t_{mn} \rangle j_{nm}$ ,  $\partial_{F_{mn}} \ln \pi_m = \langle t_{mn} \rangle A_{mn}/2$ . Using the triangle inequality for MFPTs,  $\langle t_{kn} \rangle \leq \langle t_{km} \rangle + \langle t_{mn} \rangle$  [31], we obtain bounds on the response of any state  $k$  in terms of the responses at the

ends of the perturbed edge:

$$\frac{\partial \ln \pi_n}{\partial B_{mn}} \frac{j_{mn}}{|j_{mn}|} \leq \frac{\partial \ln \pi_k}{\partial B_{mn}} \frac{j_{mn}}{|j_{mn}|} \leq \frac{\partial \ln \pi_m}{\partial B_{mn}} \frac{j_{mn}}{|j_{mn}|}, \quad (5a)$$

$$\frac{\partial \ln \pi_n}{\partial F_{mn}} \leq \frac{\partial \ln \pi_k}{\partial F_{mn}} \leq \frac{\partial \ln \pi_m}{\partial F_{mn}}, \quad (5b)$$

These inequalities reveal a fundamental localization principle: the response at any state  $k$  is bounded by the responses at the endpoints of the perturbed edge. The full range of response sensitivities can then be quantified by the sensitivity differences at the two endpoints  $m$  and  $n$ :  $|\partial_{B_{mn}} \ln(\pi_n/\pi_m)| = (\langle t_{mn} \rangle + \langle t_{nm} \rangle) |j_{mn}|$  and  $|\partial_{F_{mn}} \ln(\pi_n/\pi_m)| = (\langle t_{mn} \rangle + \langle t_{nm} \rangle) A_{mn}/2$ . To bound this range, we establish a fundamental inequality between MFPTs and edge traffic:

$$\langle t_{nm} \rangle + \langle t_{mn} \rangle \leq \frac{1}{\max[\mathcal{T}_{nm}, \mathcal{T}_{mn}]}, \quad (6)$$

where the traffic  $\mathcal{T}_{nm} = W_{nm}\pi_m$  represents the inverse average waiting time between transitions from  $m$  to  $n$ . This inequality arises because two consecutive transitions from  $m$  to  $n$  must include at least one cycle through sequential first passages ( $n \rightarrow m$  followed by  $m \rightarrow n$ ) and thus take more time on average [31]. The equal sign is taken for two-state system. Since this argument holds for transitions in both directions, we take the maximum of  $\mathcal{T}_{nm}$  and  $\mathcal{T}_{mn}$ . This bound on the first-passage cycle completing time directly yields universal bounds on the range of response sensitivities:

$$\left| \frac{\partial \ln(\pi_m/\pi_n)}{\partial B_{mn}} \right| \leq 1 - e^{-F_{\max}^{(m,n)}}, \quad \left| \frac{\partial \ln(\pi_m/\pi_n)}{\partial F_{mn}} \right| \leq 1. \quad (7)$$

Our MFPT-based approach, utilizing the thermodynamic constraint  $|\ln(\mathcal{T}_{mn}/\mathcal{T}_{nm})| \leq F_{\max}^{(m,n)}$  [32, 33] where  $F_{\max}^{(m,n)}$  is the maximum cycle affinity over all cycles containing the perturbed edge, provides a direct physical derivation of response bounds previously established using graph-theoretical methods [8]. In [8], it was shown that the first bound in (7) can be tightened to

$$|\partial_{B_{mn}} \ln(\pi_m/\pi_n)| \leq \tanh(F_{\max}^{(m,n)}/4). \quad (8)$$

However, (6) cannot be derived from (8). Using (6), tighter bounds than (7) can also be obtained by incorporating local properties of the perturbed edge, such as its current and activity (see SI [31]).

*Response precision of state observables*.— While the previous section established bounds on state probability responses, practical applications often require understanding the response of physical observables that can be measured experimentally [11, 25]. To characterize the fundamental limits on observable responses, we employ information theory to derive bounds on achievable response precision. The Fisher information associated with perturbing a parameter  $\theta$  in the steady state  $\boldsymbol{\pi}$  upper

bounds the response precision through the Cramer-Rao bound:

$$\frac{(\partial_\theta \langle \mathcal{O} \rangle)^2}{\text{Var}(\mathcal{O})} \leq I(\theta) := \sum_i \pi_i \left( \frac{\partial \ln \pi_i}{\partial \theta} \right)^2. \quad (9)$$

Here,  $\langle \mathcal{O} \rangle_\pi := \sum_i \mathcal{O}_i \pi_i$  is the steady-state average of an arbitrary observable  $\mathcal{O}$  and  $\text{Var}_\pi(\mathcal{O}) := \sum_i (\mathcal{O}_i - \langle \mathcal{O} \rangle_\pi)^2 \pi_i$  is its steady-state variance. Note that the average response sensitivity  $\sum_i \pi_i \partial_\theta \ln \pi_i = 0$  vanishes due to probability conservation, thus the Fisher information represents the variance of response sensitivity. For a bounded variable  $x \in [-a, b]$  with  $a, b > 0$  and  $\langle x \rangle = 0$ , we derive an upper bound for its variance:  $\sqrt{\text{Var}[x]} \leq \sqrt{ab} \leq (a+b)/2$ . Combined with  $I(E_m) = \pi_m(1-\pi_m) \leq 1/4$  for vertex perturbation and the range bounds from Eqs. (7), we obtain our first main result - a universal bound on response precision:

$$\frac{|\partial_X \langle \mathcal{O} \rangle_\pi|}{\sqrt{\text{Var}_\pi(\mathcal{O})}} \leq \sqrt{I(X)} \leq \frac{1}{2}. \quad (10)$$

Here,  $X$  represents the single edge or vertex perturbation. For edge-symmetric (barrier) perturbations, this bound can be further tightened using Eq. (8) to obtain

$$\frac{|\partial_{B_{mn}} \langle \mathcal{O} \rangle_\pi|}{\sqrt{\text{Var}_\pi(\mathcal{O})}} \leq \frac{\tanh(F_{\max}^{(m,n)}/4)}{2} \quad (11)$$

The bounds (10)-(11) are can be saturated by minimal two-state systems [Fig. 1]. Further tightening is possible by incorporating local properties of the perturbed edge such as current and activity (see SI [31]). The size independence of these bounds reveals that increasing system complexity cannot enhance single-perturbation response precision. However, perturbing multiple edges can achieve higher precision (Appendix A), with the precision increasing proportionally to the number of edges perturbed. These insights have important implications for biological information processing, as exemplified by the prevalence of small biochemical signaling networks which we will discuss later.

*Response of currents.*— We now extend our analysis to current observables that exhibit distinct response behaviors due to their intrinsic connection to dynamics. Using Eq. (2), we derive exact expressions for steady-state current responses and their upper bounds for three types of perturbation:

$$\frac{\partial j_{kl}}{\partial B_{mn}} = -[\delta_{(k,l)}^{(m,n)} + \Delta t_{nm}^l \mathcal{T}_{kl} - \Delta t_{nm}^k \mathcal{T}_{lk}] j_{mn}, \quad (12a)$$

$$\frac{\partial j_{kl}}{\partial F_{mn}} = [\delta_{(k,l)}^{(m,n)} + \Delta t_{nm}^l \mathcal{T}_{kl} - \Delta t_{nm}^k \mathcal{T}_{lk}] \frac{A_{mn}}{2}, \quad (12b)$$

$$\frac{\partial j_{kl}}{\partial E_m} = \pi_m j_{kl}, \quad (12c)$$

where  $\Delta t_{nm}^l := \langle t_{ln} \rangle - \langle t_{lm} \rangle$ , and  $\delta_{(k,l)}^{(m,n)} = \delta_{mk} \delta_{nl} - \delta_{ml} \delta_{nk}$  is edge delta function to distinguish local and non-local

perturbations. Then, using Eqs. (6) and (8), we obtain upper bounds for non-local and local current response as (take  $B_{kl}$  as an example)

$$\left| \frac{\partial j_{mn}}{\partial B_{kl}} \right| \leq \min \left\{ \tanh(F_{\max}^{(k,l)}/4), \frac{2|j_{kl}|}{A_{kl}} \right\} A_{mn}. \quad (13a)$$

$$\left| \frac{\partial j_{kl}}{\partial B_{kl}} \right| \leq \min \left\{ A_{kl} \tanh(F_{\max}^{(k,l)}/4), |j_{kl}| \right\} \leq A_{kl}, \quad (13b)$$

where the non-local perturbation bound is new to our knowledge and the local perturbation bound provides a complement bound that tightens the result in [15].

Thus, the single-edge response for an arbitrary current observable  $\langle \mathcal{J} \rangle := \sum_{m < n} \mathcal{J}_{mn} j_{mn}$  is upper bounded as

$$\frac{\partial \langle \mathcal{J} \rangle}{\partial B_{kl}} \leq \sum_{m < n} |\mathcal{J}_{mn}| A_{mn}. \quad (14)$$

Unlike steady-state distributions and state observables, current response is more intrinsically linked to activity. Eq. (13a)-(13b), show that higher activity leads to enhanced responses in both currents and current observables. This occurs because current observables inherently depend on jump frequencies, while state observables only depend on residence times. However, we define a type of measurable normalized current observable using the escape rates and show that their response precision is upper bounded by a size-independent constant,  $3/2$ , similar to the state observables (Appendix B).

*Nonequilibrium response theory for arbitrarily strong perturbations.*— Here, we present a novel framework for analyzing system responses to perturbations of arbitrary strength, offering enhanced experimental feasibility. We begin by generalizing Eq. (2) to cases where the perturbation can be arbitrarily strong [31]:

$$\pi'_k - \pi_k = \sum_{m < n} (\langle t_{kn} \rangle - \langle t_{km} \rangle) (\Delta W_{mn} \pi'_n - \Delta W_{nm} \pi'_m) \pi_k, \quad (15)$$

where  $\Delta W_{mn} = W'_{mn} - W_{mn}$  is the perturbation on edge  $e_{mn}$  and  $\pi'_k$  is the steady state probability of state  $k$  for perturbed dynamics. Eq. (15) reduces to Eq. (2) in the weak perturbation limit ( $|\Delta W_{mn}| \ll 1$  for all  $m, n$ ). It was recently derived in [34] using a different approach.

Using Eq. (15), we obtain the finite-perturbation counterparts of Eq. (3a) - (4) as

$$\frac{\pi'_k{}^{B'_e} - \pi_k{}^{B_e}}{1 - e^{\Delta B_e}} = (\langle t_{kn} \rangle - \langle t_{km} \rangle) \pi_k j_e^{B'_e}, \quad (16a)$$

$$\frac{\pi'_k{}^{F'_e} - \pi_k{}^{F_e}}{1 - e^{-\Delta F_e/2}} = (\langle t_{kn} \rangle - \langle t_{km} \rangle) \pi_k \left( \mathcal{T}_{mn}^{F'_e} + e^{\Delta F_e/2} \mathcal{T}_{nm}^{F'_e} \right), \quad (16b)$$

$$\frac{\pi'_k{}^{E'_m} - \pi_k{}^{E_m}}{e^{\Delta E_m} - 1} = \pi_m{}^{E'_m} (\pi_k{}^{E_m} - \delta_{km}) \quad (16c)$$

where  $\Delta B_e = B'_e - B_e$  and  $\Delta F_e = F'_e - F_e$  (for notation brevity, we denote  $e = e_{mn}$ ,  $B_e := B_{mn}$ ,  $F_e := F_{mn}$  and

$j_e := j_{mn}$  from now on). Eq. (16c) extends Eq. (4), a central result in [8], to arbitrary perturbation.

We then obtain linear relations between responses of state observables to strong and weak perturbation as

$$\frac{\langle \mathcal{O} \rangle_{\pi}^{B'_e} - \langle \mathcal{O} \rangle_{\pi}^{B_e}}{e^{\Delta B_e} - 1} = \frac{j_e^{B'_e}}{j_e^{B_e}} \partial_{B_e} \langle \mathcal{O} \rangle_{\pi}^{B_e}, \quad (17a)$$

$$\frac{\langle \mathcal{O} \rangle_{\pi}^{F'_e} - \langle \mathcal{O} \rangle_{\pi}^{F_e}}{1 - e^{-\Delta F_e/2}} = \frac{\mathcal{T}_{mn}^{F'_e} + e^{\Delta F_e/2} \mathcal{T}_{nm}^{F'_e}}{A_e^{F_e}} \partial_{F_e} \langle \mathcal{O} \rangle_{\pi}^{F_e} \quad (17b)$$

$$\frac{\langle \mathcal{O} \rangle_{\pi}^{E'_m} - \langle \mathcal{O} \rangle_{\pi}^{E_m}}{e^{\Delta E_m} - 1} = \frac{\pi_m^{E'_m}}{\pi_m^{E_m}} \partial_{E_m} \langle \mathcal{O} \rangle_{\pi}^{E_m}, \quad (17c)$$

Eq. (17a)-(17c) comprise our second main result. Our derivation of Eq. (15) relies solely on the steady-state condition and the existence of a generator pseudoinverse, and is thus not limited to Markov jump processes. Linear relations similar to Eq. (17a)-(17c) may be found for other dynamical equations.

These identities enable us to generalize nonequilibrium response theories from weak perturbation to arbitrarily strong perturbation. Our results on the precision limits of state observables are generalizable to finite perturbations by substituting Eq. (17a)-(17c) into Eq. (10)-(11). To consider the variances before and after the perturbation, an inequality first derived in [13, 19] can be applied (Appendix C).

The fluctuation-response relations for state observables derived in [23] can also be extended as:

$$\begin{aligned} \text{Cov}[\mathcal{O}_1, \mathcal{O}_2] &= \sum_e \frac{A_e}{(j_e^{B'_e})^2} \left( \frac{\Delta_{B_e} \langle \mathcal{O}_1 \rangle}{e^{\Delta B_e} - 1} \right) \left( \frac{\Delta_{B_e} \langle \mathcal{O}_2 \rangle}{e^{\Delta B_e} - 1} \right) \\ &= \sum_e \frac{A_e \left[ \frac{\Delta_{F_e} \langle \mathcal{O}_1 \rangle \Delta_{F_e} \langle \mathcal{O}_2 \rangle}{(1 - e^{-\Delta F_e/2})^2} \right]}{\left( \mathcal{T}_{mn}^{F'_e} + e^{\Delta F_e/2} \mathcal{T}_{nm}^{F'_e} \right)^2}, \end{aligned} \quad (18)$$

where  $\Delta_{B_e} \langle \mathcal{O} \rangle := \langle \mathcal{O} \rangle_{\pi}^{B'_e} - \langle \mathcal{O} \rangle_{\pi}^{B_e}$ . When  $\Delta B_e$  and  $\Delta F_e$  are small, relations in [23] are recovered. Since all terms on the right-hand side of Eq. (18) are non-negative, they provide natural lower bounds for the covariance, establishing strong-perturbation variants of fluctuation-response inequalities [17, 23]. Furthermore, applying the Cauchy-Schwartz inequality to Eq. (18) yields lower bounds for both the entropy production rate and activity [31].

Eqs. (7) and (8) can be generalized similarly to upper bound  $|\Delta_X \langle \mathcal{O} \rangle|$ , where  $X_e = B_e, F_e, E_m$ . For the  $B_e$  perturbation, two non-negative observables  $\mathcal{O}_1$  and  $\mathcal{O}_2$  satisfy (see Appendix D for proof and  $F_e$  perturbation)

$$\left| \frac{\Delta_{B_e} \langle \mathcal{O}_1 \rangle}{\langle \mathcal{O}_1 \rangle} - \frac{\Delta_{B_e} \langle \mathcal{O}_2 \rangle}{\langle \mathcal{O}_2 \rangle} \right| \leq R_{j_e} (e^{|\Delta B_e|} - 1) \tanh \left( \frac{F_{\max}^e}{4} \right), \quad (19)$$

where  $R_{j_e} = \min(j_e^{B'_e}/j_e^{B_e}, e^{\Delta B_e} j_e^{B'_e}/j_e^{B_e}) \leq 1$ . This generalizes the most general inequality in [8].  $R_{j_e} \leq 1$ , derived from (6) and (12a), recovers a finding in [15].

For steady-state currents  $j_{mn}$ , we find that for non-local responses to finite perturbation, the linearity holds similarly to steady-state probability:

$$\frac{j_{mn}^{B'_e} - j_{mn}^{B_e}}{e^{\Delta B_e} - 1} = \frac{j_{kl}^{B'_e}}{j_{kl}^{B_e}} \frac{\partial j_{mn}^{B_e}}{\partial B_{kl}}, \quad (20)$$

which is, however, not the case for local perturbations. Consequently, linearity in Eq. (17a)-(17c) does not hold for current observables  $\langle \mathcal{J} \rangle$ .

*Application: Biochemical sensing*—Cellular signaling networks must reliably detect and respond to chemical concentrations through molecular signaling networks. For edge-symmetric perturbations on an edge  $B_e$  through enzyme concentration  $[E]$ , where rates scale as  $k_{\pm} = [E]k_{\pm}^0$  and thus  $B_e \propto \ln[E]$ , we can derive a bound on sensing error through error propagation:

$$\left( \frac{\sigma_E}{[E]} \right)^2 = \left( \frac{\partial \ln[E]}{\partial B_e} \right)^2 \frac{\text{Var}_{\pi}[\mathcal{O}]}{N |\partial_{B_e} \langle \mathcal{O} \rangle_{\pi}|^2} \geq \frac{4}{N \tanh(F_c/4)^2} \quad (21)$$

where  $N$  is the number of signaling molecules,  $\sigma_E$  is the standard deviation of the enzyme concentration estimation and  $F_c$  is the cycle affinity quantifying energy dissipation. The first equality follows from the chain rule, while the inequality comes from our general bound Eq. (11). This bound on sensing error takes the same form as previously derived for specific push-pull networks [8, 35, 36], but emerges here from more general principles. It demonstrates that expanding network size and selecting observables cannot improve the performance of the fundamental limit.

To illustrate this bound in a concrete biological context, we analyze a push-pull network motif ubiquitous in cellular signaling pathways [8, 37, 38]. The substrate molecule switches between unphosphorylated state  $S$  and phosphorylated state  $S^*$  states controlled by two competing enzyme-catalyzed reactions: kinase  $K$  to transfer phosphate group (Pi) from ATP to substrate, and phosphatase  $F$  to remove the Pi. Here the barrier height is proportional to the concentration of enzymes,  $B_w \propto \ln[K]$  and  $B_k \propto \ln[F]$ , the driving force on edge  $w$  is the chemical free energy difference  $F_w \propto \mu_{\text{ATP}} - \mu_{\text{ADP}}$ . The cyclic driving force is provided by the chemical free energy of ATP hydrolysis  $F_c = \Delta\mu/k_B T$  (for reference  $\Delta\mu = \mu_{\text{ATP}} - \mu_{\text{ADP}} - \mu_{\text{Pi}}$  in cells range from 20–30  $k_B T$ ). As shown in Fig. 1, this minimal system achieves our universal bound. This provides physical insight into why cellular signaling often employs simple push-pull architectures despite evolutionary pressure for accuracy.

*Discussions.*—We have established a comprehensive theoretical framework for nonequilibrium response through MFPT, providing both exact relations and universal bounds. Our approach offers direct physical intuition while recovering and extending previous results [8, 10, 11, 15]. The framework yields two fundamental advances. First, we derive universal bounds on response precision using steady-state Fisher information, revealing a universal 1/2 upper bound for single edge or vertex

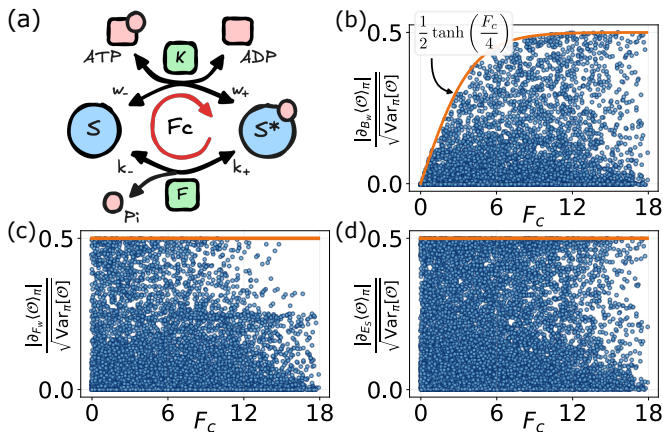


FIG. 1. (a) Minimal push-pull signaling motif where a substrate interconverts between inactive ( $S$ ) and active ( $S^*$ ) states with rates  $w_{\pm}$  and  $k_{\pm}$ , maintained out of equilibrium with cycle affinity  $F_c$ . (b-d) Numerical verification of bounds on response precision under different perturbations symmetric-edge, anti-symmetric-edge and vertex perturbations, respectively. Blue dots show numerical results for random observables and parameters; orange lines indicate theoretical upper bounds, Eqs.(10) and (11).

perturbation. Notably, our findings elucidate the role of activity in nonequilibrium response: while higher activity enables more frequent repeated measurements, thereby enhancing measurement precision of the mean value, it does not improve the intrinsic precision for state observables. From a metrological perspective, our variance is the single-measurement variance, capturing the intrinsic fluctuations of state observables. In contrast, the trajectory-wise state observables studied in recent works [17, 23], while sharing the same mean values as our state observables in the long-time limit, have variances that are tied to activity and possess the dimension of time. Our framework further reveals how current responses, though intrinsically linked to edge activities, exhibit analogous universal bounds when properly normalized. Second, we establish exact relations connecting responses across arbitrary perturbation strengths, extending the nonequilibrium response theory beyond the weak-perturbation regime, making the nonequilibrium response theory more applicable to practical experiments. Our results have direct implications for cellular sensing, where they provide physical bounds on precision independent of network architecture. Additionally, our framework can provide feasible lower bounds for the cycle force and entropy production rate [31], offering broad implications for thermodynamic inference [39–44].

Looking forward, it would be valuable to extend our theory to systems governed by Lindblad master equations. Furthermore, addressing different classes of perturbations, such as time-dependent signals commonly encountered in biological systems [45, 46], represents an important direction for future work.

## ACKNOWLEDGMENTS

R.B. was supported by JSPS KAKENHI. We are grateful to the Statistical Physics Youth Communication community for providing the initial platform for this discussion. We thank Cristian Maes, Timur Aslyamov, and Jiming Zheng for their helpful comments on the manuscript. R.B. thanks Faezeh Khodabandehlou for communications. We also acknowledge the assistance of Claude and ChatGPT for their help with writing, critical comments, and inspiring discussions.

## AUTHOR CONTRIBUTION

S.L. initiated the project and identified the response precision limit. R.B. introduced the response equalities. Both S.L. and R.B. conceptualized the study, developed the theoretical framework, completed the mathematical proofs, interpreted the results, and wrote the manuscript.

## APPENDIX

### Appendix A: Multi-edge and global perturbation

For multi-edge perturbations, the upper bound for response precision can be obtained simply by adding the contributions from each single-edge together and using the triangle inequality, for instance,

$$\begin{aligned} \frac{|\sum_{e_{mn} \in S} \partial_{B_{mn}} \langle \mathcal{O} \rangle_{\pi}|}{\sqrt{\text{Var}_{\pi}(\mathcal{O})}} &\leq \frac{1}{2} \sum_{e_{mn} \in S} \tanh(F_{\max}^{(m,n)}/4) \\ &\leq \frac{|S|}{2} \tanh(F_{\max}/4), \end{aligned} \quad (22)$$

where  $e_{mn}$  is the edge containing state  $m$ ,  $n$ ,  $S$  is the set of edges being perturbed and  $F_{\max} = \max_{e_{mn} \in S} F_{\max}^{(m,n)}$ . Thus, the optimal response precision is at most of the order of the number  $|S|$ . One may also calculate the steady-state Fisher information matrix for multi-parameter  $[I(\theta)]_{\mu\nu} = \sum_k \frac{\partial_{\theta_{\mu}} \pi_k \partial_{\theta_{\nu}} \pi_k}{\pi_k}$  and then use the multi-parameter Cramer-Rao inequality to obtain tighter bounds [17].

Additionally, for biological systems, sometimes global perturbations are more feasible. A possible choice of global perturbation is  $B_{ij}(b) \rightarrow B_{ij}(b + \epsilon)$ , where  $b$  is a physical parameter associated with all edges and  $\epsilon$  is a infinitesimal perturbation on it. Then, the corresponding Fisher information is given by

$$I(b) = \sum_{e_{mn}} (\partial_b B_{mn})^2 I(B_{mn}) \leq b_{\max}^2 \sum_{e_{mn}} I(B_{mn}), \quad (23)$$

where  $e$  is the edge and  $b_{\max} := \max_e (\partial_b B_e)$ . Thus, Eq. (10) is directly generalized to this case.

## Appendix B: Response of normalized current observables

We define a type of measurable current observable  $\langle \mathcal{J} \rangle^{nom} := \sum_{m < n} \mathcal{J}_{mn} (p_{mn} \pi_n - p_{nm} \pi_m)$  by introducing the next-state probability,

$$p_{mn} := p(x_1 = m | x_0 = n) = \frac{W_{mn}}{|W_{nn}|} \quad (m \neq n),$$

with  $x_0$  and  $x_1$  representing the states before and after a transition ( $p_{mm} := 0$ ). The normalized current observable can be interpreted as the steady-state average of an observable  $\mathcal{J}$  over the joint probability distribution  $p_{mn} \pi_n$ :  $\langle \mathcal{J} \rangle^{nom} = \sum_{m,n} \mathcal{J}_{mn} (p_{mn} \pi_n)$ , with  $\mathcal{J}_{mn} = -\mathcal{J}_{nm}$ . Thus, to characterize the response behavior  $\langle \mathcal{J} \rangle^{nom}$ , we only need to analyze the response of  $p_{mn} \pi_n$ . For simplicity, we take the perturbation on  $B_{kl}$  as an illustrative example. Recall that  $p_{kl} = \frac{W_{kl}}{|W_{ll}|}$ , so  $\partial_{B_{kl}} p_{kl} = p_{kl}(-1 - p_{kl})$  and  $\partial_{B_{lk}} p_{kl} = p_{lk}(-1 - p_{lk})$ , leading to

$$\begin{aligned} \frac{\partial \ln(p_{mn} \pi_n)}{\partial B_{kl}} &= -(\langle t_{nl} \rangle - \langle t_{nk} \rangle) j_{kl}, \quad (e_{mn} \neq e_{kl}) \\ \frac{\partial \ln(p_{kl} \pi_l)}{\partial B_{kl}} &= -1 - p_{kl} + j_{kl} \langle t_{lk} \rangle \\ \frac{\partial \ln(p_{lk} \pi_k)}{\partial B_{kl}} &= -1 - p_{lk} - j_{kl} \langle t_{kl} \rangle. \end{aligned} \quad (24)$$

The Fisher information  $I(B_{kl}) = \sum_{m,n} [\partial_{B_{kl}} \ln(p_{mn} \pi_n)]^2 (p_{mn} \pi_n)$  associated with the probability distribution  $p_{mn} \pi_n$  can be regarded as the variance of a zero-mean random variable  $\partial_{B_{kl}} \ln(p_{mn} \pi_n)$ . The triangle inequality  $-\langle t_{lk} \rangle \leq \langle t_{nl} \rangle - \langle t_{nk} \rangle \leq \langle t_{kl} \rangle$  together with (6) assure that the random variable is bounded from above and below,  $\partial_{B_{kl}} \ln(p_{mn} \pi_n) \in [-a, b]$ , with  $b + a \leq |j_{kl}|(\langle t_{kl} \rangle + \langle t_{lk} \rangle) + 1 + \max(p_{kl}, p_{lk}) \leq 3$ . Then using the idea in the main text, we have

$$I(B_{kl}) \leq \frac{a+b}{2} \leq \frac{3}{2}. \quad (25)$$

By the Cramer-Rao bound, the response precision is upper bounded as:

$$\frac{|\partial_{B_{mn}} \langle \mathcal{J} \rangle^{nom}|}{\sqrt{\text{Var}(\mathcal{J})}} \leq \frac{3}{2}, \quad (26)$$

which is not related to activity. The steady-state variance is defined as  $\text{Var}(\mathcal{J}) := \langle \mathcal{J}^2 \rangle^{nom} - (\langle \mathcal{J} \rangle^{nom})^2$ , where the average is over  $p_{mn} \pi_n$ .

## Appendix C: Additional response bounds on arbitrarily-strong perturbation

The Cramer-Rao inequality can be generalized to finite perturbation cases as [13]

$$\frac{|\langle \mathcal{O} \rangle_{\pi}^{\theta_1} - \langle \mathcal{O} \rangle_{\pi}^{\theta_0}|}{\sqrt{\text{Var}_{\pi}^{\theta_1}(\mathcal{O})} + \sqrt{\text{Var}_{\pi}^{\theta_0}(\mathcal{O})}} \leq \tanh \left( \frac{1}{2} \int_{\theta_0}^{\theta_1} \sqrt{I(\theta)} d\theta \right).$$

Combined with (10), it leads to,

$$\begin{aligned} \frac{|\langle \mathcal{O} \rangle_{\pi}^{B'_e} - \langle \mathcal{O} \rangle_{\pi}^{B_e}|}{\sqrt{\text{Var}_{\pi}^{B'_e}(\mathcal{O})} + \sqrt{\text{Var}_{\pi}^{B_e}(\mathcal{O})}} &\leq \tanh \left[ \frac{\Delta B_e \tanh \left( \frac{F_{\max}^e}{4} \right)}{4} \right], \\ \frac{|\langle \mathcal{O} \rangle_{\pi}^{F'_e} - \langle \mathcal{O} \rangle_{\pi}^{F_e}|}{\sqrt{\text{Var}_{\pi}^{F'_e}(\mathcal{O})} + \sqrt{\text{Var}_{\pi}^{F_e}(\mathcal{O})}} &\leq \tanh \left[ \frac{1}{4} \Delta F_e \right], \\ \frac{|\langle \mathcal{O} \rangle_{\pi}^{E'_m} - \langle \mathcal{O} \rangle_{\pi}^{E_m}|}{\sqrt{\text{Var}_{\pi}^{E'_m}(\mathcal{O})} + \sqrt{\text{Var}_{\pi}^{E_m}(\mathcal{O})}} &\leq \tanh \left[ \frac{1}{4} \Delta E_m \right]. \end{aligned} \quad (27)$$

which demonstrates that activity does not contribute to the response precision of state observables to strong perturbation. The single-edge finite response precision for such observables is still independent of system sizes.

## Appendix D: Proof of Eq. (19) and its asymmetric edge and vertex perturbation counterparts

Eq. (19) is derived by combining (5a), (8) and (17a). First, by using the inequality  $\min_i (x_i/y_i) \leq \sum_i x_i / \sum_i y_i \leq \max_i (x_i/y_i)$  for  $x \in \mathbb{R}$  and  $y_i \geq 0$  (at least one positive  $y_i$ ), the localization principle stated in (5a)-(5b) is generalized to arbitrary non-negative observables  $\mathcal{O}$  (assuming  $j_{mn} \geq 0$  and let  $X = B, F$ ):

$$\frac{\partial \ln \pi_n}{\partial X_{mn}} \leq \frac{\partial \ln \langle \mathcal{O} \rangle}{\partial X_{mn}} \leq \frac{\partial \ln \pi_m}{\partial X_{mn}}, \quad (28)$$

which together with (7) and (8) yield

$$\left| \frac{\partial \ln(\langle \mathcal{O}_1 \rangle / \langle \mathcal{O}_2 \rangle)}{\partial B_{mn}} \right| \leq \tanh \frac{F_{\max}^{(m,n)}}{4}, \quad \left| \frac{\partial \ln(\langle \mathcal{O}_1 \rangle / \langle \mathcal{O}_2 \rangle)}{\partial F_{mn}} \right| \leq 1,$$

which were derived in [8, 10] using algebraic graph theory. Applying (17a) and (17b) gives Eq. (19) and

$$\left| \frac{\Delta F_e \langle \mathcal{O}_1 \rangle}{\langle \mathcal{O}_1 \rangle} - \frac{\Delta F_e \langle \mathcal{O}_2 \rangle}{\langle \mathcal{O}_2 \rangle} \right| \leq R_{A_e} (e^{\Delta F_e} - e^{\Delta F_e/2}), \quad (29)$$

where  $R_{A_e} := \frac{\mathcal{T}_{mn}^{F'_e} + e^{\Delta F_e/2} \mathcal{T}_{nm}^{F'_e}}{e^{\Delta F_e} A_e^{F_e}} \leq 1$  ( $\Delta F_e \geq 0$ ).  $R_{A_e} \leq 1$  is shown below by calculating the responses of  $\mathcal{T}_{mn}$  and  $\mathcal{T}_{nm}$  to perturbation on  $F_{mn}$ :

$$\begin{aligned} \frac{\partial \ln(\mathcal{T}_{mn})}{\partial F_{mn}} &= \frac{1}{2} (1 - \langle t_{nm} \rangle A_{mn}), \\ \frac{\partial \ln(\mathcal{T}_{nm})}{\partial F_{mn}} &= \frac{1}{2} (-1 + \langle t_{mn} \rangle A_{mn}). \end{aligned} \quad (30)$$

With (6), they are bounded as,

$$-\frac{1}{2} \leq \frac{\partial \ln(\mathcal{T}_{mn})}{\partial F_{mn}} \leq \frac{1}{2}, \quad -\frac{1}{2} \leq \frac{\partial \ln(\mathcal{T}_{nm})}{\partial F_{mn}} \leq \frac{1}{2}, \quad (31)$$

which reproduce the result in [15] for activity response.

- 
- [1] R. Kubo, The fluctuation-dissipation theorem, Reports on Progress in Physics **29**, 255 (1966).
- [2] Y. Cao and S. Liang, Stochastic thermodynamics for biological functions, Quantitative Biology **13**, e75 (2025).
- [3] P. R. ten Wolde, N. B. Becker, T. E. Ouldridge, and A. Mugler, Fundamental Limits to Cellular Sensing, Journal of Statistical Physics **162**, 1395 (2016).
- [4] H. Qian, Phosphorylation Energy Hypothesis: Open Chemical Systems and Their Biological Functions, Annual Review of Physical Chemistry **58**, 113 (2007).
- [5] H. Ge, M. Qian, and H. Qian, Stochastic theory of nonequilibrium steady states. Part II: Applications in chemical biophysics, Physics Reports Stochastic Theory of Nonequilibrium Steady States (Part II): Applications in Chemical Biophysics, **510**, 87 (2012).
- [6] L. Peliti and S. Pigolotti, *Stochastic Thermodynamics: An Introduction* (Princeton University Press, 2021).
- [7] A. Dechant and S.-i. Sasa, Fluctuation–response inequality out of equilibrium, Proceedings of the National Academy of Sciences **117**, 6430 (2020).
- [8] J. A. Owen, T. R. Gingrich, and J. M. Horowitz, Universal Thermodynamic Bounds on Nonequilibrium Response with Biochemical Applications, Physical Review X **10**, 011066 (2020).
- [9] J. A. Owen, P. Talla, J. W. Biddle, and J. Gunawardena, Thermodynamic bounds on ultrasensitivity in covalent switching, Biophysical Journal **122**, 1833 (2023).
- [10] J. A. Owen and J. M. Horowitz, Size limits the sensitivity of kinetic schemes, Nature Communications **14**, 1280 (2023).
- [11] G. Fernandes Martins and J. M. Horowitz, Topologically constrained fluctuations and thermodynamics regulate nonequilibrium response, Physical Review E **108**, 044113 (2023).
- [12] C. Maes, Response Theory: A Trajectory-Based Approach, Frontiers in Physics **8**, 229 (2020).
- [13] Y. Hasegawa, Unifying speed limit, thermodynamic uncertainty relation and Heisenberg principle via bulk-boundary correspondence, Nature Communications **14**, 2828 (2023).
- [14] T. Aslyamov and M. Esposito, General Theory of Static Response for Markov Jump Processes, Physical Review Letters **133**, 107103 (2024).
- [15] T. Aslyamov and M. Esposito, Nonequilibrium Response for Markov Jump Processes: Exact Results and Tight Bounds, Physical Review Letters **132**, 037101 (2024).
- [16] K. Ptaszyński, T. Aslyamov, and M. Esposito, Dissipation Bounds Precision of Current Response to Kinetic Perturbations, Physical Review Letters **133**, 227101 (2024).
- [17] E. Kwon, H.-M. Chun, H. Park, and J. S. Lee, Fluctuation-response inequalities for kinetic and entropic perturbations (2024), arXiv:2411.18108 [cond-mat].
- [18] P. E. Harunari, S. Dal Cengio, V. Lecomte, and M. Poletti, Mutual Linearity of Nonequilibrium Network Currents, Physical Review Letters **133**, 047401 (2024).
- [19] Y. Hasegawa, Thermodynamic Correlation Inequality, Physical Review Letters **132**, 087102 (2024).
- [20] T. Aslyamov, K. Ptaszyński, and M. Esposito, Nonequilibrium fluctuation-response relations: From identities to bounds, arXiv preprint arXiv:2410.17140 (2024).
- [21] K. Liu and J. Gu, Dynamical activity universally bounds precision of response (2024), arXiv:2410.20800 [cond-mat].
- [22] J. Zheng and Z. Lu, Universal Non-equilibrium Response Theory Beyond Steady States (2024), arXiv:2403.10952 [cond-mat].
- [23] K. Ptaszyński, T. Aslyamov, and M. Esposito, Nonequilibrium Fluctuation-Response Relations for State Observables (2024), arXiv:2412.10233 [cond-mat].
- [24] J. Zheng and Z. Lu, Spatial correlation unifies nonequilibrium response theory for arbitrary markov jump processes, arXiv preprint arXiv:2501.01050 (2025).
- [25] H.-M. Chun and J. M. Horowitz, Trade-offs between number fluctuations and response in nonequilibrium chemical reaction networks, The Journal of Chemical Physics **158**, 174115 (2023).
- [26] G. Lan, P. Sartori, S. Neumann, V. Sourjik, and Y. Tu, The energy–speed–accuracy trade-off in sensory adaptation, Nature Physics **8**, 422 (2012).
- [27] Y. Tu and W.-J. Rappel, Adaptation in living systems, Annual review of condensed matter physics **9**, 183 (2018).
- [28] C. D. Meyer, Jr., The Condition of a Finite Markov Chain and Perturbation Bounds for the Limiting Probabilities, SIAM Journal on Algebraic Discrete Methods **1**, 273 (1980).
- [29] G. E. Cho and C. D. Meyer, Markov chain sensitivity measured by mean first passage times, Linear Algebra and its Applications **316**, 21 (2000).
- [30] S. E. Harvey, S. Lahiri, and S. Ganguli, Universal energy-accuracy tradeoffs in nonequilibrium cellular sensing, Physical Review E **108**, 014403 (2023).
- [31] See supplemental materials for analytical derivations and mathematical details.
- [32] S. Liang and S. Pigolotti, Thermodynamic bounds on time-reversal asymmetry, Physical Review E **108**, L062101 (2023).
- [33] S. Liang, P. De Los Rios, and D. M. Busiello, Thermodynamic Bounds on Symmetry Breaking in Linear and Catalytic Biochemical Systems, Physical Review Letters **132**, 228402 (2024).
- [34] F. Khodabandehlou, C. Maes, and K. Netočný, Affine relationships between steady currents (2024), arXiv:2412.05019 [cond-mat].
- [35] C. C. Govern and P. R. Ten Wolde, Energy Dissipation and Noise Correlations in Biochemical Sensing, Physical Review Letters **113**, 258102 (2014).
- [36] C. C. Govern and P. R. ten Wolde, Optimal resource allocation in cellular sensing systems, Proceedings of the National Academy of Sciences **111**, 17486 (2014).
- [37] G. Li and H. Qian, Sensitivity and Specificity Amplification in Signal Transduction, Cell Biochemistry and Biophysics **39**, 45 (2003).
- [38] W. Bialek and S. Setayeshgar, Physical limits to biochemical signaling, Proceedings of the National Academy of Sciences **102**, 10040 (2005).
- [39] U. Seifert, From Stochastic Thermodynamics to Thermodynamic Inference, Annual Review of Condensed Matter Physics **10**, 171 (2019).
- [40] P. E. Harunari, A. Dutta, M. Poletti, and E. Roldán, What to learn from a few visible transitions’ statistics?, Phys. Rev. X **12**, 041026 (2022).

- [41] J. van der Meer, B. Ertel, and U. Seifert, Thermodynamic inference in partially accessible markov networks: A unifying perspective from transition-based waiting time distributions, *Phys. Rev. X* **12**, 031025 (2022).
- [42] A. C. Barato and U. Seifert, Thermodynamic uncertainty relation for biomolecular processes, *Phys. Rev. Lett.* **114**, 158101 (2015).
- [43] T. R. Gingrich, J. M. Horowitz, N. Perunov, and J. L. England, Dissipation bounds all steady-state current fluctuations, *Phys. Rev. Lett.* **116**, 120601 (2016).
- [44] J. M. Horowitz and T. R. Gingrich, Thermodynamic uncertainty relations constrain non-equilibrium fluctuations, *Nature Physics* **16**, 15 (2020).
- [45] G. Nicoletti and D. M. Busiello, Information propagation in multilayer systems with higher-order interactions across timescales, *Phys. Rev. X* **14**, 021007 (2024).
- [46] G. Nicoletti, M. Bruzzone, S. Suweis, M. Dal Maschio, and D. M. Busiello, Information gain at the onset of habituation to repeated stimuli, *eLife* **13**, 10.7554/eLife.99767.1 (2024).